Korean J. Chem. Eng., 40(12), 2855-2865 (2023)
DOI: 10.1007/s11814-023-1410-6

pISSN: 0256-1115
eISSN: 1975-7220

Comprehensive analysis of acid gases on mercury removal by $CuCl_2$ modified char exposure to oxy-fuel environment: Experiment and XPS perception

Qingshan Zeng*,, Hui Wang*,**,†, Jingmao Wu*,**, Hengyuan Ran*,**, Kang Yang*,**, and Jianfei Wu*****

*MIIT Key Laboratory of Thermal Control of Electronic Equipment, School of Energy and Power Engineering, Nanjing University of Science and Technology, Nanjing, China, 210094
**Advanced Combustion Laboratory, School of Energy and Power Engineering, Nanjing University of Science and Technology, Nanjing, China, 210094
***China UNITED Gas Turbine Technology., Ltd., Shanghai, China, 201306
(*Received 4 January 2023 • Revised 12 February 2023 • Accepted 2 March 2023*)

Abstract−In this work, 0.15 mol/L $CuCl_2$ solution was used to impregnate rice husk char. Experiments were conducted in a laboratory-scale fixed-bed reactor to investigate the oxidation mechanism of Hg^0 by acidic gases. The effects of acid gases (SO_2, HCl and NO) atmospheres on the mercury removal efficiency of the adsorbent were studied by FTIR, XPS and experiments. The FTIR results showed that the surface of the prepared rice husk char adsorbent contained a large amount of Cu^{2+} and chlorine-containing functional groups. The XPS results showed that the Cu^+ on the surface of the adsorbent increased after mercury adsorption. This work shows that the inhibitory effect of SO_2 on Hg removal is reflected in the blockage of the pore structure on the adsorbent surface; the competitive adsorption of O_2 needed for the generation of C-O*, the formation of an acid mist by SO_2 hinders the contact of Hg^0 with the active site. The promotion of HCl is due to the production of active chlorine substances (Cl*) to promote the oxidation of Hg^0 to HgCl, $HgCl_2$ and HgO. And introduction of NO will react with O_2, while generation of NO_2 is beneficial to the oxidation of Hg^0 to HgO and $Hg(NO_3)_2$. The optimum mercury removal efficiency of the adsorbent is nearly 100% under certain conditions.

Keywords: Mercury, Oxy-fuel Combustion, Biomass Char, $CuCl_2$, Acid Gases

INTRODUCTION

Mercury has attracted widespread attention due to its volatility, indigestibility, accumulation in the global environment and neurotoxicity to humans [1-3]. In 2013, the Global Mercury Assessment Technical Background Report stated that the utilization of coal in coal-fired power plants is a significant source of mercury emissions [4]. In October of the same year, the Minamata Convention on Mercury was signed by over 140 countries [5].

The main forms of mercury in the flue gas emitted by coal-fired power plants are: particulate bound mercury (Hg^P), gaseous elemental mercury (Hg^0) and gaseous oxidized mercury (Hg^{2+}) [6-8]. Existing pollutant control equipment, including desulfurization and particulate removal units, more easily captures particulate mercury (Hg^P) and divalent mercury (Hg^{2+}) [9-11]. While Hg^0 is more unstable and insoluble within water, it is considered to be the key to mercury removal [12,13]. Sorbent injection technology is an important means of mercury removal in coal-fired power plants [14]. In coal-fired electricity production, activated carbon injection technology is commonly utilized [15]. It has been shown to be useful in the removal of mercury [16,17]. However, due to the high production cost, high price, and low recycling rate of activated carbon, the application is greatly restricted [18,19]. Biomass materials have a wide range of sources, abundant resources and good regeneration performance, and are natural materials for making carbon-based adsorbents [20-22]. However, the biomass carbon material has a very limited adsorption capacity for mercury; it is usually treated by chemical modification methods to improve the mercury removal effect of the biomass carbon [23-25].

Existing studies have shown that the modification of carbon-based materials impregnated with $CuCl_2$ can effectively improve the mercury removal efficiency. Zhang et al. [26] synthesized $CuCl_2$/AC by impregnating $CuCl_2$ on an activated carbon (AC) support, showing excellent Hg^0 removal efficiency over 90%. Xiao et al. [27] studied the adsorption and oxidation properties of $CuCl_2$-MF for Hg^0 under different conditions. Under the optimal conditions, using $CuCl_2$-MF injection combined with existing pollutant control devices, the total mercury removal efficiency rate reached 98.72%. Chen et al. [28] investigated the mercury removal performance of $CuCl_2$ modified activated carbon. The effects of operating parameters and gas composition were investigated. It was found that $CuCl_2$-AC exhibited excellent mercury removal performance under various conditions compared with the raw activated carbon.

There are still few studies on the mercury removal mechanism of copper salt modified char in acid gas in oxy-fuel combustion atmosphere. To obtain the mercury removal mechanism of rice husk coke containing copper under oxy-fuel combustion atmosphere, this work focuses on the effect of acid gas in flue gas under

†To whom correspondence should be addressed.
E-mail: wanghui22@njust.edu.cn

oxy-fuel combustion atmosphere on the mercury removal performance of rice husk coke containing copper, and analyzes the physical and chemical properties of adsorbent before and after the reaction by using FTIR, XPS and other characterization techniques. The novelty of this work is to explore the modification of agricultural waste rice husk coke with copper chloride to prepare a high-efficiency mercury removal adsorbent with mercury removal efficiency of more than 95% under certain conditions, and to study the mercury removal mechanism of the adsorbent under different acidic atmospheres, providing theoretical support for the development of biomass mercury removal adsorbent. This study adopts this method because of the need in the oxy-fuel combustion atmosphere and the lack of relevant conditions in previous studies.

EXPERIMENT AND METHOD

1. Adsorbent Preparation

The origin of the raw materials used in the experiment is Nanjing, Jiangsu. These rice husks were repeatedly washed with deionized water and dried in a drying oven. Then the rice husks were crushed with a crusher, and the biomass in the size between them was sieved with a standard sieve of 50 mesh and 150 mesh. Then the sieved biomass powder was put in a crucible, then put it into a muffle furnace, and pyrolysis was performed at 600 °C for 10-15 minutes, then the crucible was taken out and opened for cooling to obtain the corresponding biomass char. A standard sieve was used to get the 70-140 mesh original rice husk char. A mixed solution of $CuCl_2$ and rice husk char was prepared, and the mixed solution was stirred with a magnetic stirrer for 6 h, then allowed to stand for 6 h. Then the mixed solution was filtered, the Cu-containing rice husk char was washed with deionized water until the liquid under the funnel was colorless; the washed char sample was put into a constant temperature drying oven, and dried at 80 °C for 6 h. Finally, after the Cu-containing rice husk char was cooled, the samples were bagged and kept for future use. The concentration of $CuCl_2$ used in the preparation of Cu-containing rice husk char was 0.15 mol/L, the ratio of rice husk char to $CuCl_2$ solution is 1 g: 50 ml, which was marked as RHC-Cl1.5.

2. Experimental Apparatus

This experiment was carried out on a fixed bed mercury adsorption experimental platform as shown in Fig. 1. The experimental platform is mainly composed of the following parts: mercury vapor generating device, gas distribution system, tube furnace, mercury analyzer and exhaust gas purification device. The adsorbent is dispersed on a glass tube through quartz wool, and the glass tube is installed in a tube furnace. The length of the glass tube is 1,100 mm and the diameter is 20 mm. Ar is used as the carrier gas and the balance gas of the system. The carrier gas carries the mercury vapor generated by the water bath into the flue gas mixer to mix it with other gases. The function of the balance gas is to keep the total flow of the experimental flue gas unchanged; Ar is an inert gas and will not participate in the reaction of the experiment. The tube furnace temperature was set to 150 °C during the reaction. Mercury analyzer model was QM208B. The total gas flow rate was 2 L/min, and the initial mercury vapor release was 54.4 μg/m^3 in the experiment. The experimental measurement time is 2 h. The specific experimental atmosphere working conditions are shown in Table 1.

Table 1. Experimental conditions

Test	Atmosphere
1	70%CO_2+6%O_2+300ppmSO_2
2	70%CO_2+6%O_2+600ppmSO_2
3	70%CO_2+6%O_2+900ppmSO_2
4	70%CO_2+6%O_2+10ppmHCl
5	70%CO_2+6%O_2+20ppmHCl
6	70%CO_2+6%O_2+30ppmHCl
7	70%CO_2+6%O_2+400ppmNO
8	70%CO_2+6%O_2+800ppmNO
9	70%CO_2+6%O_2+1200ppmNO
10	70%CO_2+6%O_2

3. Evaluation Index of Adsorbent Adsorption Performance

The mercury breakthrough rate η can reflect the mercury removal performance of the adsorbent under different experimental conditions, which is calculated by Eq. (1) [29].

$$\eta = \frac{C_0^{out}}{C_0^{in}} \times 100\% \quad (1)$$

C_0^{out} is Hg^0 concentration at the reactor outlet, μg/m^3; C_0^{in} is Hg^0 concentration at the reactor inlet, μg/m^3.

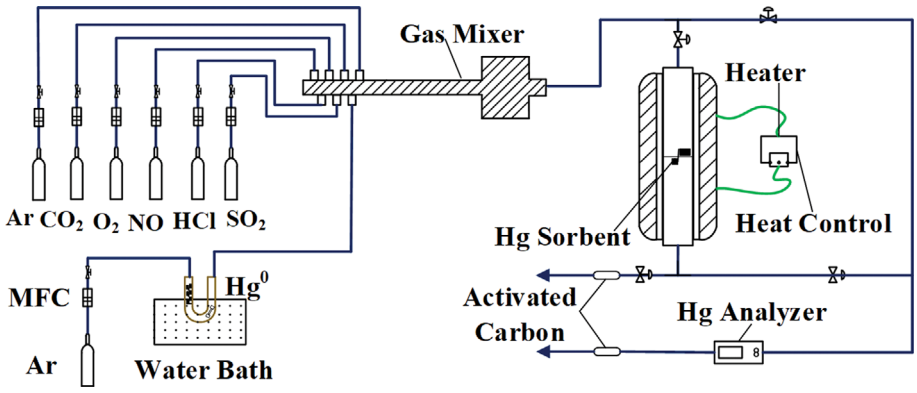

Fig. 1. Schematic diagram of the mercury adsorption experimental platform.

The mercury uptake per unit of mercury provides a good estimate of the performance of the adsorbent for mercury per gram. The precise equation is provided by Eq. (2).

$$m = \frac{QC_{in}}{M}\int_0^t (1-\eta_r)d\tau \quad (2)$$

where t stands for the test time, between 0 to 120, min; η_τ is the breakthrough rate at τ; Q is the total stream of the gas, L/min; M is the weight of the adsorbent that was utilized during the study, g; m, the accumulated adsorption capacity for each gram of adsorbent from 0 to t, μg/g.

RESULTS AND DISCUSSION

1. Sorbent Characterization

To analyze the changes of oxygen-containing functional groups on the surface of the samples during the modification process, the samples before and after modification were characterized by FTIR. Fig. 2 shows the results of FTIR spectroscopy analysis of rice husk char before and after modification. The fluctuation at 892 cm^{-1} is attributed to the C-O-C absorption peak [30], and the peak at 1,065 cm^{-1} is attributed to the stretching vibration of C-O and C-Cl [31], indicating that the active Cl in the modified solution was successfully loaded into the rice. The shock at 1,248 cm^{-1} is attributed to C-O stretching [32], 1,394 cm^{-1} is -COOH [33], 2,988 cm^{-1} and 2,901 cm^{-1} are C-H stretching shocks [34,35]. The peak

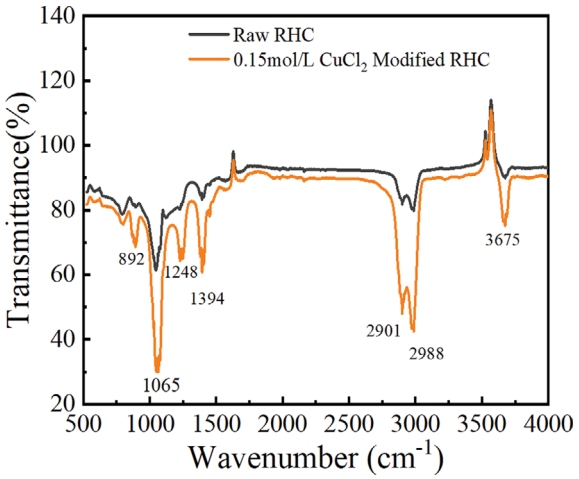

Fig. 2. FTIR analysis of rice husk char before and after modification.

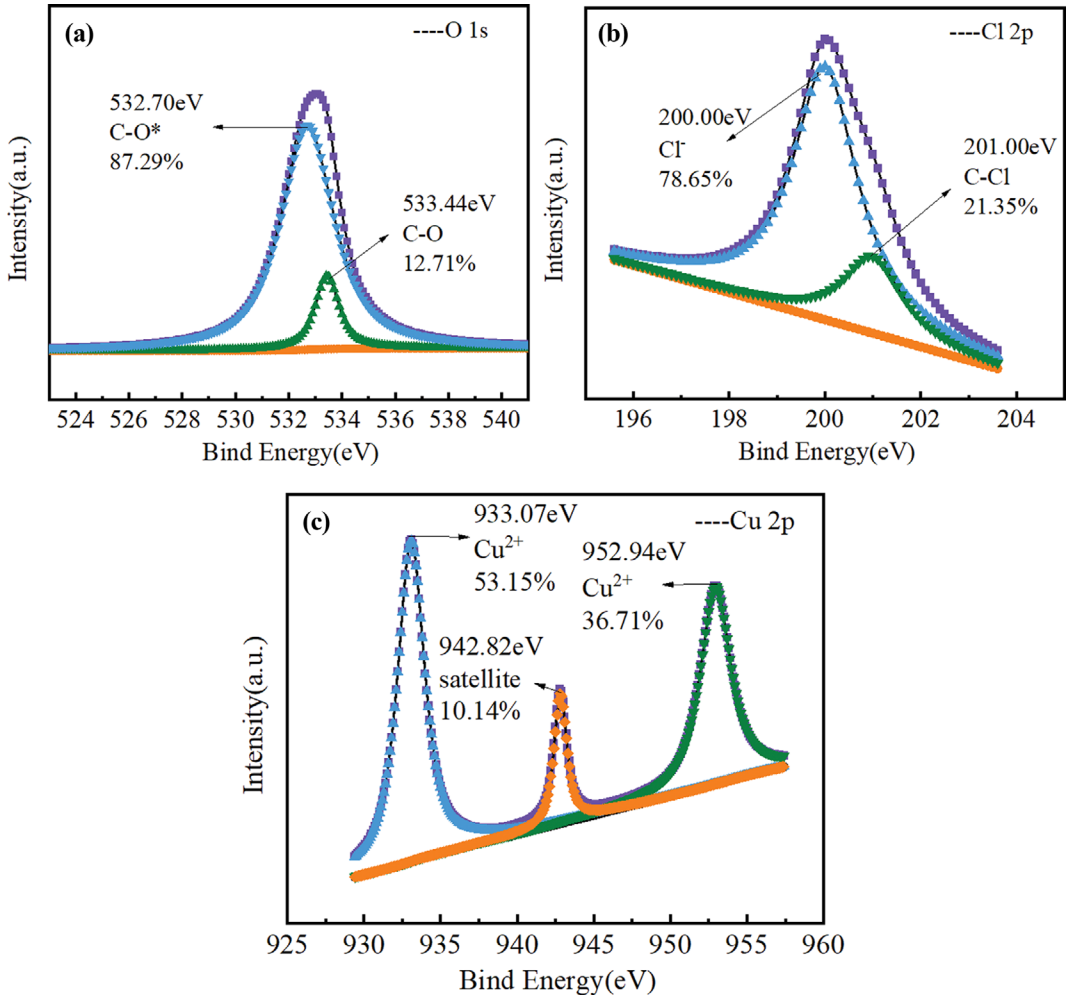

Fig. 3. XPS spectra of RHC-Cl1.5.

at 3,675 cm^{-1} is attributed to the vibration of -OH [36]. The formation of -OH contributes to the increase of chemisorbed O and can facilitate the removal of Hg by ligand exchange [37]. It can be seen that the number of oxygen-containing functional groups on the surface of the sample after immersion in the modified solution has been greatly improved, and these oxygen-containing functional groups are beneficial to the removal of Hg^0.

X-ray photoelectron spectroscopy (XPS) analysis of O 1s, Cl 2p and Cu 2p of the modified adsorbent is shown in Fig. 3. It can be seen from the figure that the surface of the adsorbent modified by $CuCl_2$ impregnation was successfully loaded with chemisorption oxygen (C-O*), C-Cl and Cu^{2+}, and these functional groups have been proved to be beneficial for the removal of mercury [29,38].

2. Effect of SO_2 on Mercury Removal

On the basis of 70%CO_2+6%O_2 atmosphere, the mercury removal experiments were carried out by adding SO_2 with concentrations of 300 ppm, 600 ppm and 900 ppm, respectively. The mercury breakthrough rate curves of different SO_2 concentrations are shown in Fig. 4. Mercury uptake of different SO_2 concentration is shown in Fig. 5.

It can be seen from Fig. 4 that when SO_2 with concentrations of 300 ppm and 600 ppm is added, the mercury penetration rate decreases to 40% in the first 10 minutes and then remains stable in the following 110 minutes. The mercury penetration rate after two hours is 32.73% and 34.95%, respectively. The difference between the two stabilized mercury penetration rates is very small: only 2.22%. When the SO_2 concentration increased to 900 ppm, the mercury penetration rate maintained a slight downward trend after falling to 67.74% in the 8th min, and the final value was 56.45%. At this time, the mercury removal efficiency of the adsorbent was greatly inhibited.

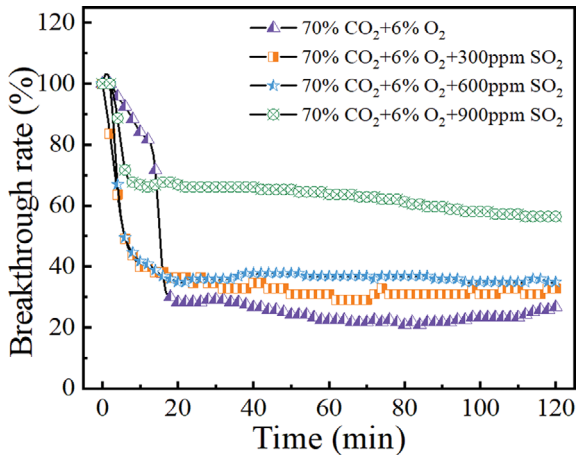

Fig. 4. Mercury breakthrough rate of different SO_2 introduction.

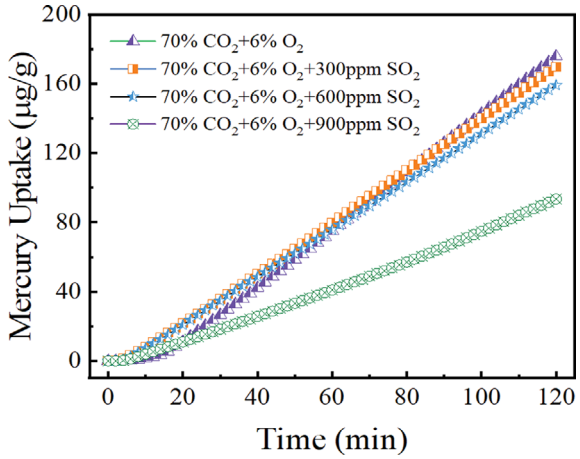

Fig. 5. Mercury uptake of different SO_2 introduction.

It can be seen from Fig. 5 that after two hours, the cumulative adsorption amount of mercury unit at the concentration of 300 ppm and 600 ppm SO_2 was 170.00 μg/g and 159.31 μg/g, respectively. The difference between the two is 10.69 μg/g, with little difference. When the SO_2 concentration increased to 900 ppm, the mercury unit cumulative adsorption decreased to 93.53 μg/g, the difference from 600 ppm SO_2 was 65.78 μg/g, and the decrease ratio was 41.29%. It can be seen that the high concentration of SO_2 has a more obvious inhibitory effect on the removal of mercury.

It can be found that with the increase of SO_2 concentration, the mercury breakthrough rate gradually increases and the mercury uptake gradually decreases in the experiment. Therefore, it can be concluded that SO_2 has an inhibitory effect on the mercury removal of rice husk char. While the effect of 300 ppm and 600 ppm concentrations of SO_2 on mercury removal efficiency was not significant, the inhibition effect of SO_2 at 900 ppm concentration on mercury adsorption was more obvious. The reason for this phenomenon may be due to the dual effect of SO_2 on mercury removal. On the one hand, SO_2 will be oxidized to form SO_3 in the presence of O_2, and SO_3 can further interact with Hg^0 to form stable $HgSO_4$ [39]. The reaction equations are described by Eqs. (3)-(4) [40]. On the other hand, SO_2 may have an adverse effect on the removal of Hg^0 through the following ways: one is to block the pore structure on the surface of rice husk char, which hinders the adsorption of Hg^0 on the surface of the adsorbent [41]. The second is to compete with Hg^0 for the active site of oxidation, weakening the oxidation process of Hg^0 [42]. At low concentrations, the promoting effect of SO_2 can offset part of the inhibitory effect, so the inhibitory effect is not obvious, which is why the inhibitory effect is more obvious at high concentrations. This is similar to the conclusion of Wu et al. [43].

$$SO_2 + 1/2O_2 \rightarrow SO_3 \quad (3)$$

$$Hg^0 + 1/2O_2 + SO_3 \rightarrow HgSO_4 \quad (4)$$

To further elucidate the effect of SO_2 on the mercury removal process of rice husk char modified by $CuCl_2$, the O 1s, Cl 2p, Cu 2p, S 2p and Hg 4f were characterized on the used adsorbent surface by XPS; the results were shown in Fig. 6.

For O 1s, the wave crest located at 531.9 eV, 533.2 eV was connected with chemical adsorbed oxygen (C-O*) [44] and C-O [45]. After mercury adsorption, the C-O* content on the adsorbent surface decreased from 87.29% to 47.49%, and the C-O content increased from 12.71% to 52.51%. This indicates that the adsorbent combines with oxygen in the environment to generate C-O*, and C-O* participates in the oxidation process of Hg and partially converts to C-O. The reaction equations are described by Eqs. (5)-

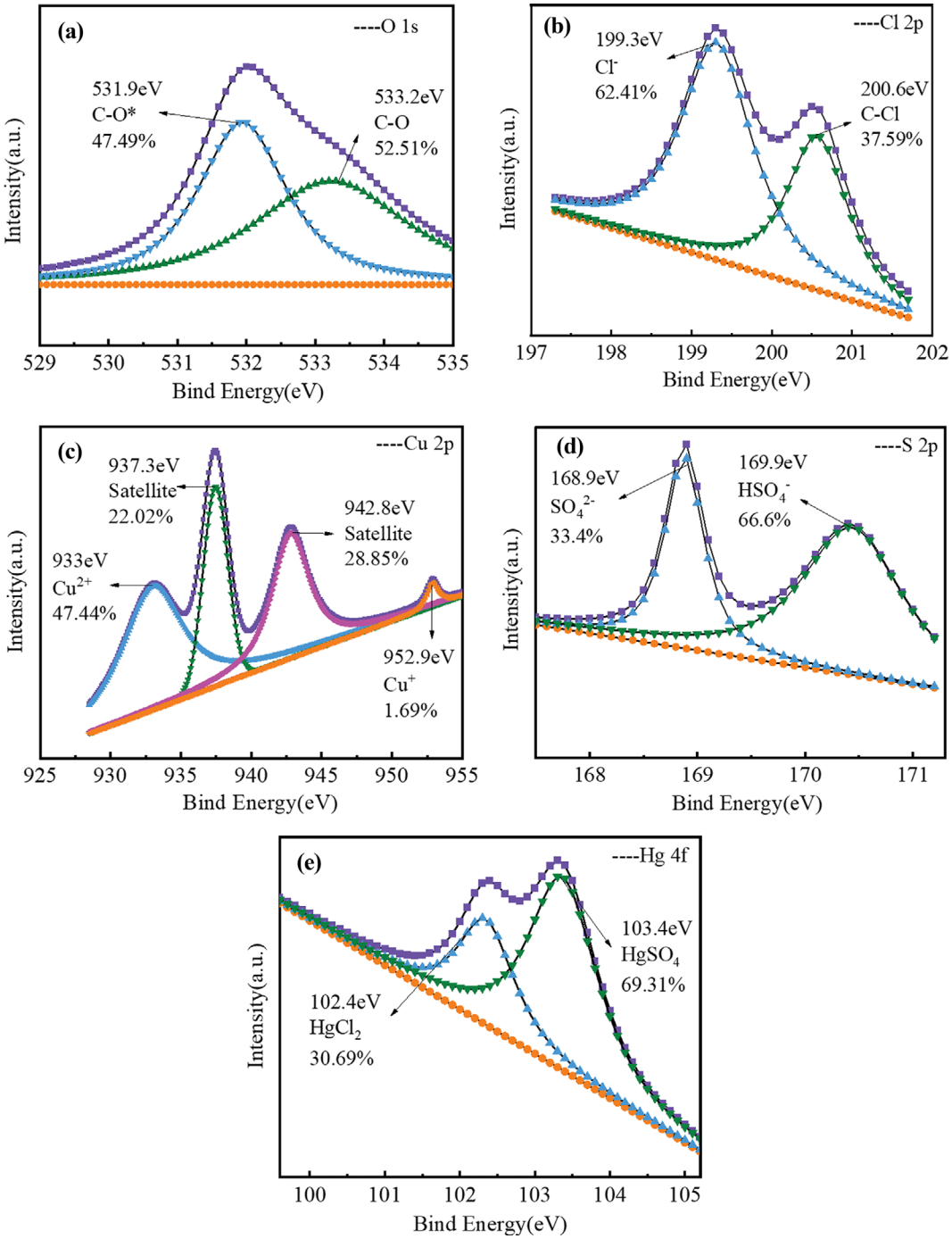

Fig. 6. XPS spectra of RHC-Cl1.5 used adsorbent in SO_2 environment.

(6) [46,47].

$$2C + O_2 \rightarrow 2C\text{-}O^* \quad (5)$$

$$C\text{-}O^* + Hg \rightarrow HgO + C \quad (6)$$

For Cl 2p, the peak at 199.3 eV was attributed to Cl^- [48], peak at 200.6 eV belonged to C-Cl groups [49]. Compared with the adsorbent before adsorption, the Cl^- content decreased from 78.65% to 62.41%, and the C-Cl content increased from 21.35% to 37.59%. Some studies [50,51] have shown that the C-Cl groups may provide an active site to oxidize Hg^0 to be HgCl and $HgCl_2$, and convert to Cl^- during the reaction of Hg^0. Further, in the presence of O_2 and SO_2, $HgCl_2$ can be converted into a more stable $HgSO_4$ [52]. The reaction equations are described by Eqs. (7)-(11) [53,54]. The process of converting $HgCl_2$ to $HgSO_4$ will generate Cl_2, which in turn reacts with O in the environment to generate Cl species, the Cl species and C generate C-Cl functional groups again, which can explain why the content of C-Cl increases after adsorbent.

$$Cl + C \rightarrow C\text{-}Cl \quad (7)$$

$$Hg + C\text{-}Cl \rightarrow HgCl + C \quad (8)$$

$$HgCl + C\text{-}Cl \rightarrow HgCl_2 + C \quad (9)$$

$$HgCl_2 + O_2 + SO_2 \rightarrow HgSO_4 + Cl_2 \quad (10)$$

$$O + Cl_2 \rightarrow ClO + Cl \quad (11)$$

For Cu 2p, the wave peaks at 933 eV, 937.3 eV, 942.8 eV and 952.9 eV are attributed to Cu^+, satellite peak, satellite peak and Cu^+, respectively [55-57]. The content of Cu^{2+} nearly disappears. It is speculated that the oxidation mechanism of $CuCl_2$ to Hg^0 is as follows: Hg^0 is oxidized by lattice Cl in $CuCl_2$; this process reduces $CuCl_2$ to CuCl [58].

For S 2p, the peaks detected at 168.9 eV and 169.9 eV are attributed to SO_4^{2-} [59] and HSO_4^- [60], respectively. It is confirmed that SO_2 will be oxidized in oxy-fuel atmosphere and $HgSO_4$ may be generated. For Hg 4f, the peaks of 102.4 eV and 103.4 eV are attributed to the presence of $HgCl_2$ and $HgSO_4$ [61,62]. This can prove the occurrence of the reaction process of Eqs. (9) and (10).

In summary, the inhibitory effect of SO_2 on Hg removal may be achieved by the following ways: from the physical level analysis, SO_2 tends to block the pore structure of the adsorbent surface, which hinders the reaction of Hg^0 with the active sites on the adsorbent surface. From the chemical level analysis, one is that SO_2 generates competitive adsorption of O_2 needed in the process of generating C-O*, and the other is that HSO_4^- generated by SO_2 tends to form a layer of acid mist covering the adsorbent surface, which will hinder the contact between Hg^0 and $CuCl_2$ and weaken the oxidation of Hg^0, tending to block the carbon surface with O_2, creating a barrier to the generation of oxygen-containing functional groups such as C-O*.

3. Effect of HCl on Mercury Removal

On the basis of 70%CO_2+6%O_2 atmosphere, the mercury removal experiments were carried out by adding HCl with concentrations of 10 ppm, 20 ppm and 30 ppm, respectively. The mercury breakthrough rate curves of different HCl concentrations are shown in Fig. 7. Mercury uptake of different HCl concentration is shown in Fig. 8.

As can be seen from Fig. 7, compared with before the addition,

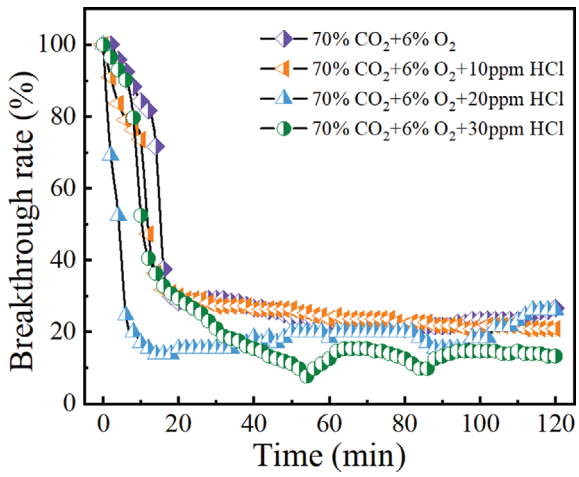

Fig. 7. Mercury breakthrough rate of different HCl introduction.

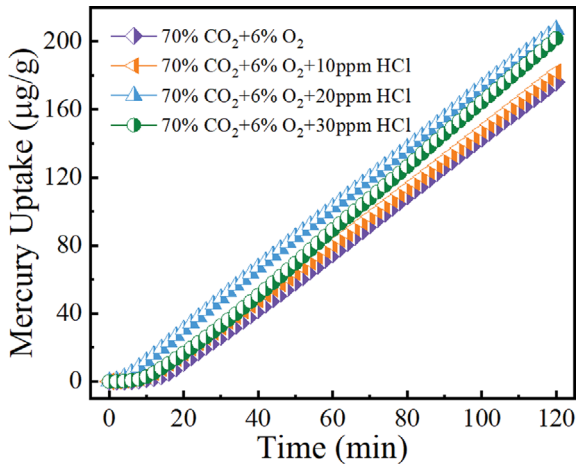

Fig. 8. Mercury uptake of different HCl introduction.

there is a slight decrease in the mercury breakthrough rate in the first 16 min after the addition of 10 ppm HCl, but the trend of both mercury breakthrough rate curves is basically flat in the following 104 min. While the mercury breakthrough rate decreases significantly in the first 60 min after the addition of 20 ppm HCl. After adding 30 ppm HCl, the mercury breakthrough rate was higher than that of the 20 ppm condition in the first 36 min; it remained low after 36 min. The minimum mercury penetration rate reaches 7.7%, but its penetration rate decreases slowly until 38 min, which is lower than other conditions.

It can be seen from Fig. 8 that with the increase of HCl, the mercury uptake of the $CuCl_2$ modified rice husk char adsorbent gradually increased. And the adsorption amount did not increase much when 10 ppm was added compared with that not added, from 175.89 μg/g increased to 181.93 μg/g, the increment was only 6.04 μg/g. The adsorption amount when 30 ppm was added was 206.89 μg/g; the increment was 31 μg/g. The mercury uptake rate of the 20 ppm in the first 36 minutes is far less than that of the 30 ppm, so it shows that the mercury uptake rate of the former is higher than that of the latter in 2 h. It may be that high concentration blocked the pore structure of the adsorbent, which caused the decrease of mercury removal efficiency.

To further elucidate the effect of HCl on the mercury removal process of rice husk char modified by $CuCl_2$, the O 1s, Cl 2p, Cu 2p and Hg 4f were characterized on the used adsorbent surface by XPS; the results are shown in Fig. 9.

For O 1s, the peaks detected at 531.4 eV and 533.3 eV are attributed to C-O* and C-O, respectively [63,64]. After the adsorption experiment, the C-O* content on the adsorbent surface decreased from 87.29% to 60.89%, while the C-O content increased from 12.71% to 39.11%. It indicates that C-O* was involved in the oxidation process of Hg^0 and new C-O functional groups were generated.

For Cl 2p, the peak positions at 200.3 eV and 201.5 eV correspond to Cl^- and C-Cl [65,66]. The Cl^- content decreased from 78.65% to 75.4%, while the C-Cl content increased from 21.35% to 24.6%. Although the oxidation process of Hg may consume C-Cl, the HCl in the atmosphere will supplement the C-Cl, so the C-Cl content on the surface of the adsorbent after the reaction

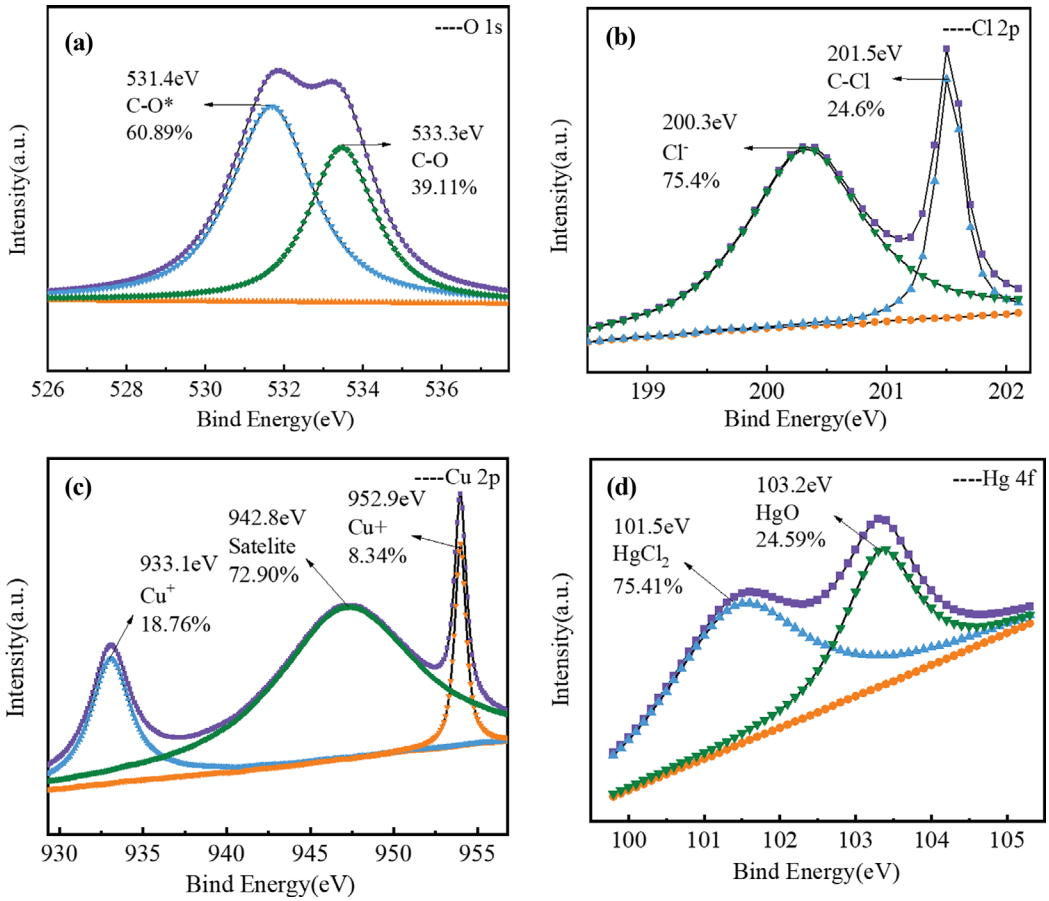

Fig. 9. XPS spectra of RHC-Cl1.5 used adsorbent in HCl environment.

increases instead. The HCl in the atmosphere is first adsorbed on the surface of the adsorbent, then the HCl dissociates to form active chlorine species (Cl*), and Cl* further reacts with Hg^0 to form $HgCl_2$. The possible reaction process is as follows: Eq. (12)-(14) [67].

$$HCl \rightarrow H + Cl^* \quad (12)$$

$$Hg + Cl^* \rightarrow HgCl \quad (13)$$

$$HgCl + Cl^* \rightarrow HgCl_2 \quad (14)$$

For Cu 2p, the peaks detected at 933.1 eV, 942.8 eV and 952.9 eV are attributed to Cu^+, satellite peak and Cu^+, respectively [68-70]. The content of Cu^{2+} is not detected, indicating that Cu^{2+} participated in the oxidation process of Hg^0. For Hg 4f, the peaks at 101.5 eV and 103.2 eV are due to the presence of $HgCl_2$ and HgO [71,72].

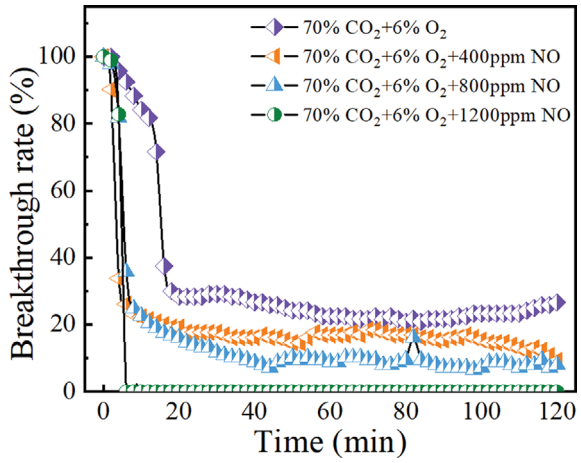

Fig. 10. Mercury breakthrough rate of different NO introduction.

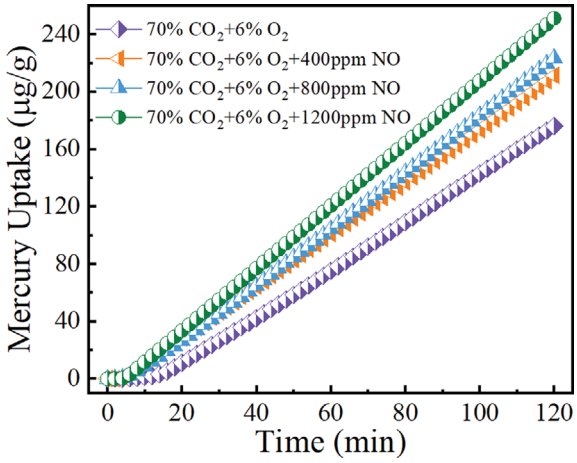

Fig. 11. Mercury uptake of different NO introduction.

4. Effect of NO on Mercury Removal

On the basis of 70%CO_2+6%O_2 atmosphere, the mercury removal experiments were carried out by adding NO with concentrations of 400 ppm, 800 ppm and 1,200 ppm, respectively. The mercury breakthrough rate curves of different NO concentrations are shown in Fig. 10. Mercury uptake of different NO concentration is shown in Fig. 11.

It can be seen from Fig. 10 that the mercury breakthrough rate of Cu-containing rice husk char can reach the steady state more quickly when NO is added to the flue gas. Under the flue gas without NO, the mercury penetration rate of Cu-containing rice husk char started to stabilize at 18 min, and its lowest value was 20.8%, which was higher than that of the flue gas with NO. When 400 ppm NO was introduced, the stabilization time of mercury breakthrough rate was advanced to 8 min, and fluctuated around 16.2% from 8 min to 98 min with a range of less than 1.5%. After that, the mercury breakthrough decreased gradually, and the minimum of 9.2% was obtained at the end of the experiment. When the NO

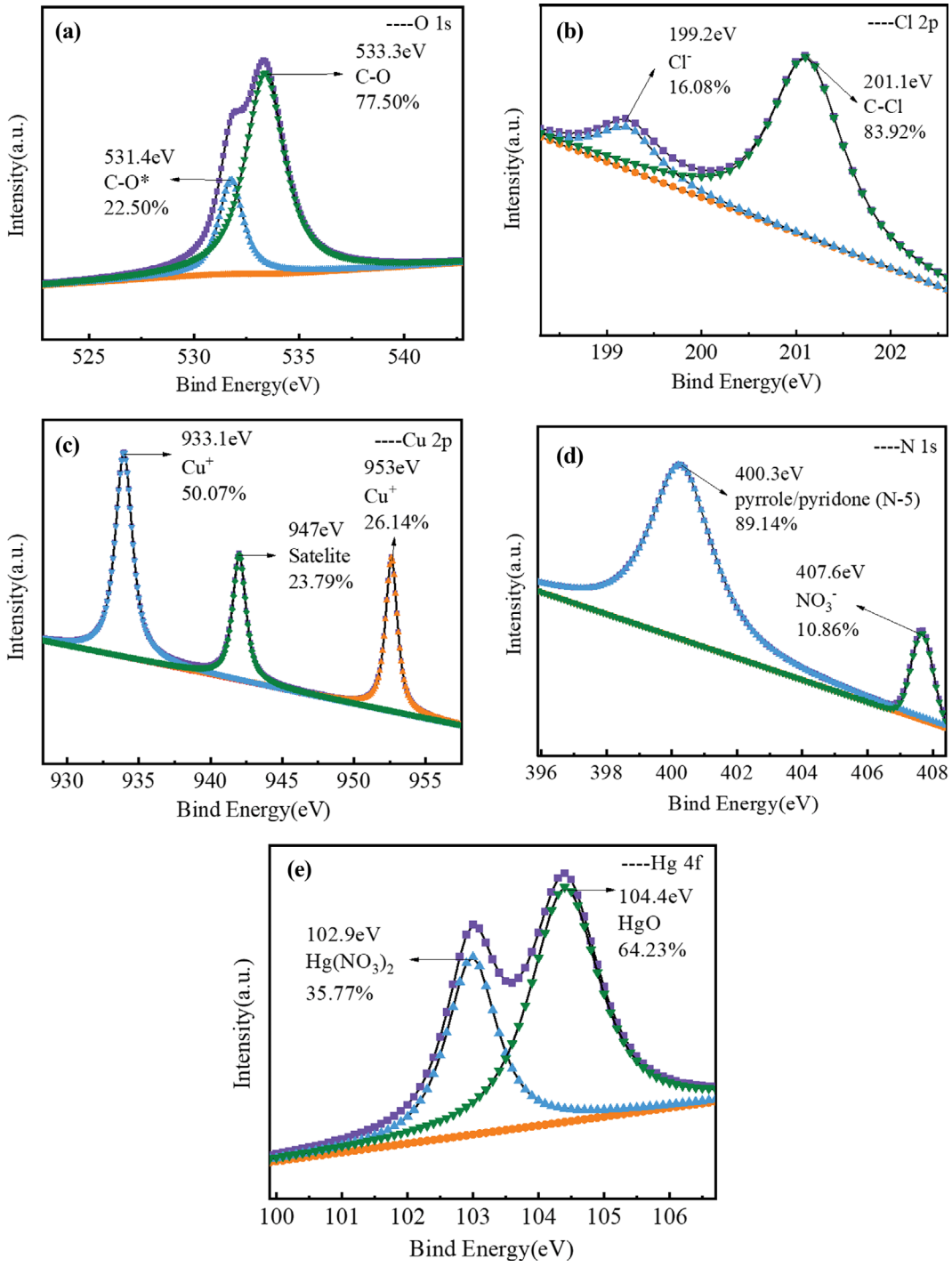

Fig. 12. XPS spectra of RHC-Cl1.5 used adsorbent in NO environment.

concentration was 800 ppm, mercury breakthrough rate was also stable around 8 min, but in the first 44 min, the mercury penetration rate gradually decreased and reached the lowest value of 7.3%, and then slowly increased and fluctuated. With the increase of NO concentration to 1,200 ppm, the decrease of mercury breakthrough rate was more obvious, and the efficiency of mercury removal from the adsorbent reached more than 95% after 4 min of the experiment.

As shown in Fig. 11, the addition of NO improved the mercury uptake of the Cu-containing rice husk char, and this improvement increased with the increase of NO concentration. At the end of the experiment, the mercury uptake of nitrogen-free flue gas was the lowest, which was 175.9 μg/g, accounting for 67.4% of the input mercury mass. With the increase of NO concentration, the mercury uptake of Cu-containing rice husk char increased. When the NO concentration in the flue gas was 400 ppm, the mercury uptake of mercury per unit was 211.3 μg/g, which is 35.4 μg/g higher than that of the nitrogen-free flue gas, accounting for 80.9% of the input mercury mass. When the NO concentration increased to 800 ppm, the mercury uptake t only increased by 12.1 μg/g, which was close to the adsorption amount at 400 ppm NO. When the NO concentration reached the maximum of 1,200 ppm, the mercury uptake increased by 27.6 μg/g to 251 μg/g, which accounted for 96.1% of the input mercury mass.

To further elucidate the effect of NO on the mercury removal process of rice husk char modified by $CuCl_2$, the O 1s, Cl 2p, Cu 2p, N 1s and Hg 4f were characterized on the used adsorbent surface by XPS; the results are shown in Fig. 12.

For O 1s, the wave peaks at 531.4 and 533.3 are associated with C-O* and C-O, respectively [71,73]. Note that the content of C-O* in NO atmosphere (22.50%) is much less than that in SO_2 (47.49%) and HCl (60.89%) atmosphere, which may be the result of competition between NO and C-O* formation process for O_2. NO_2 can promote the oxidation of Hg^0 and is also beneficial to the removal of mercury Hg^0. As shown in Eq. (15)-(17) [74,75].

$$2NO + 2O_2 + 6Hg \rightarrow N_2 + 6HgO \quad (15)$$

$$2NO + O_2 \rightarrow 2NO_2 \quad (16)$$

$$NO_2 + Hg \rightarrow NO + HgO \quad (17)$$

For Cl 2p and Cu 2p, the content of C-Cl did not change much before and after adsorption, indicating that in the NO atmosphere, C-Cl hardly participated in the oxidation process of mercury, and the content of Cu^{2+} all disappeared too. The main role was played by NO. As shown in Eq. (18) [76]. Since $Hg(NO_3)_2$ is volatile, it is speculated that it may be released from the reactor in the form of gas phase at the experimental temperature [77], which may be the reason for the lower content of NO_3^- and $Hg(NO_3)_2$ detected on the N 1s and Hg 4f spectra.

$$Hg + 2NO_2 + O_2 \rightarrow Hg(NO_3)_2 \quad (18)$$

CONCLUSION

In this work, 0.15 mol/L $CuCl_2$ solution was used to impregnate rice husk char. The results of Fourier transform infrared spectroscopy (FTIR) and X-ray photoelectron spectroscopy (XPS) showed that the amount of oxygen-containing functional groups and chlorine species on the surface of the samples after immersion was greatly improved. The effects of SO_2, HCl and NO atmospheres on the mercury removal efficiency of the adsorbent were studied by experiments and XPS. The results showed that high concentrations of SO_2 inhibited the mercury removal efficiency of the adsorbent. While the mercury removal efficiency gradually increased with the increase of HCl and NO concentrations.

In SO_2 atmosphere, the main mercury products are $HgCl_2$ and $HgSO_4$. At low concentrations, the promoting effect of SO_2 can offset part of the inhibitory effect, so the inhibitory effect is not obvious, which is why the inhibitory effect is more obvious at high concentrations.

In HCl atmosphere, the HCl in the atmosphere is first adsorbed on the surface of the adsorbent, then the HCl dissociates to form Cl species, and the formed Cl species further reacts with Hg^0 to form $HgCl_2$.

In NO atmosphere, NO is oxidized by O_2 to NO_2, which can promote the oxidation of Hg^0, which is beneficial to the removal of Hg^0. The main mercury products are HgO and $Hg(NO_3)_2$.

The presence of O_2 in the environment can supplement the consumption of C-O*, and NO may compete with the formation of C-O* for O_2. C-Cl and C-O*, facilitating the removal of Hg^0 and converting Hg^0 into $HgCl_2$ and HgO.

ACKNOWLEDGEMENTS

This work was supported by the National Natural Science Foundation of China (51706104), National Natural Science Foundation of Jiangsu Province (BK20211370) and the Fundamental Research Funds for the Central Universities (30920031103).

Competing Interests

The authors have no relevant financial or non-financial interests to disclose.

Author Contributions

Qingshan Zeng: Writing - Original Draft, Visualization.
Hui Wang: Project administration, Supervision, Funding acquisition.
Jingmao Wu: Writing - Review & Editing, Formal analysis.
Hengyuan Ran: Writing - Review & Editing, Formal analysis.
Kang Yang: Writing - Review & Editing, Investigation.
Jianfei Wu: Conceptualization, Methodology, Investigation.

REFERENCES

1. S. Alex, *J. Environ. Health Sci.*, **4**(2), 37 (2018).
2. D. Ye, X. Wang, R. Wang, S. Wang, H. Liu and H. Wang, *J. Environ. Chem. Eng.*, **9**(5), 105993 (2021).
3. S. Zhao, H. Luo, A. Ma, W. Xie, K. Sun and Z. Sun, *Fuel*, **313**, 122979 (2022).
4. M. P. Ancora, L. Zhang, S. Wang, J. J. Schreifels and J. Hao, *Energy Policy*, **88**, 485 (2016).
5. Z. Wang, J. Liu, Y. Yang, S. Miao and F. Shen, *Energy Fuels*, **32**(4), 4453 (2018).

6. J. Yang, H. Xu, Y. Zhao, H. Li and J. Zhang, *Energy Fuels*, **35**(5), 3581 (2021).
7. C. Li, Y. Duan, H. Tang, C. Zhu, Y.-n. Li, Y. Zheng and M. Liu, *Fuel*, **211**, 621 (2018).
8. S. Zhao, D. Pudasainee, Y. Duan, R. Gupta, M. Liu and J. Lu, *Prog. Energy Combust. Sci.*, **73**, 26 (2019).
9. Y. Li, J. Yu, Y. Liu, R. Huang, Z. Wang and Y. Zhao, *J. Hazard. Mater.*, 128132 (2022).
10. H. Ran, H. Wang, J. Wu, Y. Zhu, J. Wu and H. Shen, *Ind. Eng. Chem. Res.*, **60**(48), 17450 (2021).
11. J. Wu, H. Wang, H. Shen, C. Shen, Y. Zhu, J. Wu and H. Ran, *Ind. Eng. Chem. Res.*, **60**(33), 12200 (2021).
12. Y. Wang, J. Ni, P. Chen, J. Chen, F. Jia and S. Song, *Phys. E: Low-dimensional Systems and Nanostructures*, **127**, 114504 (2021).
13. A. Zhang, W. Zheng, J. Song, S. Hu, Z. Liu and J. Xiang, *Chem. Eng. J.*, **236**, 29 (2014).
14. A. Shen, Y. Wang, R. Wang, Y. Duan, J. Tao, X. Gu, P. Wang and Z. Xu, *Fuel*, **326**, 124990 (2022).
15. Q. Zhou, Y. Duan, M. Chen, M. Liu, P. Lu and S. Zhao, *Chem. Eng. J.*, **345**, 578 (2018).
16. X. Zhang, Y. Li, Z. Zhang, M. Nie, L. Wang and H. Zhang, *Sci. Total Environ.*, **778**, 146245 (2021).
17. A. Ma, S. Zhao, H. Luo, Z. Sun, X. Xie, Y. Liao, X. Liang and H. Li, *Chem. Eng. J.*, **429**, 132154 (2022).
18. Y. Peng, T. Wang, Y. Gu, J. Wang, Y. Zhang and W.-P. Pan, *Fuel*, **301**, 121054 (2021).
19. S. Zhao, Y. Liao, X. Xie, Y. Wang and Z. Sun, *Chem. Eng. J.*, **450**, 138023 (2022).
20. D. Liu, C. Li, J. Wu and Y. Liu, *Chem. Eng. J.*, **391**, 123514 (2020).
21. S. Zhao, H. Luo, A. Ma, W. Xie, K. Sun and Z. Sun, *Chem. Eng. J.*, **435**, 135073 (2022).
22. H. Shen, H. Zhang, Y. Xu, H. Chen, Y. Zhu, Z. Zhang and W. Li, *Energy Conv.*, **269**, 116116 (2022).
23. M. Mariana, A. K. HPS, E. Mistar, E. B. Yahya, T. Alfatah, M. Danish and M. Amayreh, *J. Water Process Eng.*, **43**, 102221 (2021).
24. Y. Li, Y. Liu, W. Yang, L. Liu and J. Pan, *Fuel*, **291**, 120152 (2021).
25. C. Zhao, X. Chen and C. Zhao, *Ind. Eng. Chem. Res.*, **50**(8), 4464 (2011).
26. J. Zhang, C. Li, X. Du, L. Gao, S. Li, Y. Zhang, Z. Li and Y. Yi, *Environ. Sci. Pollut. Res.*, **27**(15), 17891 (2020).
27. R. Xiao, T. Gao, X. Cui, Y. Ji, Y. Zhang, X. Chuai, Z. Xiong, Y. Liao, H. Gu and J. Yang, *Fuel*, **310**, 122219 (2022).
28. Y. Chen, H. Liu, X. Guo, F. Wu, Y. Zhao and J. Zhang, *Ind. Eng. Chem. Res.*, **59**(13), 5557 (2020).
29. C. Shen, H. Wang, H. Shen, J. Wu, Y. Zhu, W. Shi, X. Zhang and Z. Ying, *Energy Fuels*, **34**(8), 9872 (2020).
30. S. C. Agwuncha, S. Owonubi, D. P. Fapojuwo, A. Abdulkarim, T. P. Okonkwo and E. M. Makhatha, *Mater. Today: Proc.*, **38**, 958 (2021).
31. B. Hinterstoisser, M. Åkerholm and L. Salmén, *Carbohydr. Res.*, **334**(1), 27 (2001).
32. G. F. Huang, Q. T. Wu, J. W. C. Wong and B. B. Nagar, *Bioresour. Technol.*, **97**(15), 1834 (2006).
33. W. Yan, J. Zhang and C. Jing, *J. Colloid Interface Sci.*, **390**(1), 196 (2013).
34. K. Yadav, R. Bagal, S. Parmar, T. U. Patro and A. C. Abhyankar, *Ind. Eng. Chem. Res.*, **60**(39), 14225 (2021).
35. A. Abd-Elhamid, A. Nayl, A. A. E. Shanshory, H. M. Soliman and H. Aly, *RSC Adv.*, **9**(10), 5770 (2019).
36. M. Consumi, G. Leone, G. Tamasi and A. Magnani, *Food Additives Contam.: Part A*, **38**(10), 1629 (2021).
37. Y. Huang, J. Tang, L. Gai, Y. Gong, H. Guan, R. He and H. Lyu, *Chem. Eng. J.*, **319**, 229 (2017).
38. M. Lv, G. Q. Luo, R. J. Zou, Q. Y. Ji, C. Fang, L. Wang, X. Li and H. Yao, *Fuel*, **322**, 124229 (2022).
39. H. Li, Y. Wang, S. Wang, X. Wang and J. Hu, *Fuel*, **208**, 576 (2017).
40. S. Tao, C. Li, X. Fan, G. Zeng, P. Lu, X. Zhang, Q. Wen, W. Zhao, D. Luo and C. Fan, *Chem. Eng. J.*, **210**, 547 (2012).
41. J. Zhang, C. T. Li, X. Y. Du, S. H. Li and L. Huang, *Fuel*, **324**, 9 (2022).
42. J. Luo, Q. Niu, M. Jin, Y. Cao, L. Ye and R. Du, *J. Hazard. Mater.*, **376**, 21 (2019).
43. S.-j. Wu, R. Katayama, M. Azhar Uddin, E. Sasaoka and Z.-m. Xie, *Energy Fuels*, **29**(10), 6598 (2015).
44. Y. Li, Y. X. Liu, W. Yang, L. Liu and J. F. Pan, *Fuel*, **291**, 120152 (2021).
45. T. Yao, Y. Duan, T. M. Bisson, R. Gupta, D. Pudasainee, C. Zhu and Z. Xu, *J. Hazard. Mater.*, **374**, 267 (2019).
46. J. F. Ma, C. T. Li, L. K. Zhao, J. Zhang, J. K. Song, G. M. Zeng, X. N. Zhang and Y. Xie, *Appl. Surf. Sci.*, **329**, 292 (2015).
47. Z. Zhou, X. Liu, Y. Hu, J. Xu, X. E. Cao, Z. Liao and M. Xu, *Fuel*, **225**, 134 (2018).
48. K. Feng, Y. Zhang, Z. G. Li, C. W. Yao, L. Yao and C. Y. Fan, *Surf. Coat. Tech.*, **397**, 126004 (2020).
49. J. Gu, P. Shao, L. Luo, Y. Wang, T. Zhao, C. Yang, P. Chen and F. Liu, *Sep. Purif. Technol.*, **285**, 120377 (2022).
50. H. W. Zhang, H. J. Shi, J. Y. Chen, K. Zhao, L. Wang and Y. H. Hao, *Korean J. Chem. Eng.*, **33**(11), 3134 (2016).
51. Q. Q. Shi, X. Zhang, B. X. Shen, K. Ren, Y. T. Wang and J. Z. Luo, *Chem. Eng. J.*, **406**, 126828 (2021).
52. W. Du, L. B. Yin, Y. Q. Zhuo, Q. S. Xu, L. Zhang and C. H. Chen, *Ind. Eng. Chem. Res.*, **53**(2), 582 (2014).
53. B. Zhang, X. Zeng, P. Xu, J. Chen, Y. Xu, G. Luo, M. Xu and H. Yao, *Environ. Sci. Technol.*, **50**(21), 11837 (2016).
54. J. R. Edwards, R. K. Srivastava and J. D. Kilgroe, *J. Air Waste Manage.*, **51**(6), 869 (2001).
55. X. Zhou, W. Xu, H. Wang, L. Tong, H. Qi and T. Zhu, *Chem. Eng. J.*, **254**, 82 (2014).
56. H. Yi, Q. Yu, X. Tang, P. Ning, L. Yang, Z. Ye and J. Song, *Ind. Eng. Chem. Res.*, **50**(7), 3960 (2011).
57. F. Matloubi Moghaddam, R. Pourkaveh and M. Ahangarpour, *ChemistrySelect*, **3**(9), 2586 (2018).
58. Z. J. Zhou, X. W. Liu, Y. C. Hu, Z. Q. Liao, S. Cheng and M. H. Xu, *Fuel*, **216**, 356 (2018).
59. X. Zhang, Z. Li, J. Wang, B. Tan, Y. Cui and G. He, *Fuel*, **203**, 308 (2017).
60. J. Xie, Z. Qu, N. Yan, S. Yang, W. Chen, L. Hu, W. Huang and P. Liu, *J. Hazard. Mater.*, **261**, 206 (2013).
61. R. L. Hao, X. H. Wang, Y. H. Liang, Y. J. Lu, Y. M. Cai, X. Z. Mao, B. Yuan and Y. Zhao, *Chem. Eng. J.*, **330**, 1279 (2017).
62. R. Hao, X. Dong, Z. Wang, L. Fu, Y. Han, B. Yuan, Y. Gong and Y. Zhao, *Environ. Sci. Technol.*, **53**(14), 8324 (2019).
63. W. Yang, Y. X. Liu, Q. Wang and J. F. Pan, *Chem. Eng. J.*, **326**, 169

(2017).
64. W. Yang, Y. Li, S. Shi, H. Chen, Y. Shan and Y. X. Liu, *Fuel*, **256**, 115977 (2019).
65. T. Gao, Y. Zhang, Y. Qiu, Z. Xiong, J. Yang, Y. Zhao and J. Zhang, *Sci. China Technol. Sci.*, **64**(11), 2441 (2021).
66. G. J. Lan, Q. F. Ye, Y. N. Zhu, H. D. Tang, W. F. Han and Y. Li, *Acs Appl. Nano Mater.*, **3**(3), 3004 (2020).
67. T. Liu, C. Y. Man, X. Guo and C. G. Zheng, *Fuel*, **173**, 209 (2016).
68. B. Xu, W.-Y. Shi, W. Sun, L.-M. Pan and Y.-Q. Dong, *Appl. Surf. Sci.*, 565 (2021).
69. Y. Chen, X. Guo, F. Wu, Y. Huang and Z. Yin, *Appl. Surf. Sci.*, **458**, 790 (2018).
70. W. Xu, Y. G. Adewuyi, Y. Liu and Y. Wang, *Fuel Process. Technol.*, **170**, 21 (2018).
71. B. Shen, S. Zhu, X. Zhang, G. Chi, D. Patel, M. Si and C. Wu, *Fuel*, **224**, 241 (2018).
72. R. L. Hao, Z. Qian, X. J. Yang, M. C. Luo, X. H. Feng, W. T. Qiao, Y. Zhao and B. Yuan, *Chem. Eng. J.*, **450**, 137997 (2022).
73. W. Yang, Z. Y. Liu, W. Xu and Y. X. Liu, *Fuel*, **214**, 196 (2018).
74. H. C. Zhang, T. Wang, Y. S. Zhang, B. M. Sun and W. P. Pan, *J. Cleaner Prod.*, **257**, 120598 (2020).
75. C. M. Zhang, W. Song, X. C. Zhang, R. Li, S. J. Zhao and C. M. Fan, *J. Mater. Sci.*, **53**(13), 9429 (2018).
76. S. S. Tao, C. T. Li, X. P. Fan, G. M. Zeng, P. Lu, X. Zhang, Q. B. Wen, W. W. Zhao, D. Q. Luo and C. Z. Fan, *Chem. Eng. J.*, **210**, 547 (2012).
77. Y. Li, P. D. Murphy, C. Y. Wu, K. W. Powers and J. C. Bonzongo, *Environ. Sci. Technol.*, **42**(14), 5304 (2008).